Hollow Core–Shell Mesospheres of Crystalline SnO_2 Nanoparticle Aggregates for High Capacity Li^+ Ion Storage

Da Deng and Jim Yang Lee*

Department of Chemical & Biomolecular Engineering, Faculty of Engineering, National University of Singapore, 10 Kent Ridge Crescent, Singapore 119260

Received October 25, 2007. Revised Manuscript Received January 6, 2008

Crystalline SnO_2 nanoparticles were successfully assembled into a higher-order nanostructure of hollow core–shell mesospheres by a simple and environmentally benign procedure consisting of solvothermal synthesis and postsynthesis calcination. Carbon mesospheres laden with crystalline SnO_2 nanoparticles were formed, using a suitably formulated water−ethanol mixture, as the sole product of solvothermal synthesis from tin and carbon precursors. Subsequent calcination compressed the SnO_2 nanoparticles into stable hollow core–shell mesospheres. The carbon in the mesospheres played the constructive role of templating the final product morphology during the carbon removal process. This method of preparation is simple, low cost, and could be conveniently scaled up for volume production. This unique SnO_2 nanostructure could store an exceedingly large amount of Li^+, and it cycled well as a phase-pure SnO_2 anode.

Introduction

Wide band semiconducting SnO_2 is used in a diverse range of applications.[1–13,24] It is believed that some applications may actually benefit from a properly designed SnO_2 nanostructure. While SnO_2 can now be synthesized as nanowires,[10] nanorods,[11] nanotubes,[12] nanobelts,[13] and nanooctahedra;[3] the organized assembly of low-dimensional nanounits (e.g., SnO_2 nanoparticles) into higher-order structures (e.g., hollow core–shell particles) where the integrated geometry may lead to functional improvements, remains a challenge. For example, SnO_2 would be a good substitute for the carbon anode in lithium-ion batteries if its high Li^+ storage capacity (782 vs 372 mAh/g for graphite) is not undermined by limited cyclability. Nanostructured SnO_2 has been suggested as a possible solution to this application problem.[1,2,22–24] It will be intellectually stimulating and technologically important to determine whether a higher-order design of the nanostructure could lead to improvements in application performance, while keeping the method of preparation relatively simple and scalable.

Template-assisted synthesis and solvothermal synthesis are currently the two most common methods of preparation of hollow nanostuctures.[1–4,14–18] Template-assisted synthesis relies on the template to sculpt the product morphology. It offers ease of morphology control through template selection. A number of removable templates can be used to generate simple hollow nanostructures.[1,4,14–17] However, template-assisted synthesis is not without problems: difficulty in template fabrication, the possibility of product deconstruction during the template removal process, the shortage of templates for generating hollow structures with complex interiors, and multistep and costly operations. By comparison, solvothermal synthesis has notable advantages such as simple and straightforward operations and low-cost, scaleable production. It has been successfully used in the preparation of hollow spheres,[2] hollow octahedra,[3] and hollow boxes.[18] The morphology of nanostructures obtained by solvothermal methods is strongly dependent on the solvents used, the ions involved, acidity, and other environmental factors.[2,3,18] Quite unlike template-assisted synthesis, there is no good method to predict the product morphology a priori in a solvothermal synthesis.

A procedure that combined template-assisted and solvothermal syntheses was used here to form hollow core–shell mesospheres of crystalline SnO_2 nanoparticle aggregates for lithium ion battery applications. The procedure was devel-

* To whom correspondence should be addressed. E-mail: cheleejy@nus.edu.sg.

(1) Han, S.; Jang, B.; Kim, T.; Oh, S. M.; Hyeon, T. *Adv. Funct. Mater.* **2005**, *15*, 1845.
(2) Lou, X. W.; Wang, Y.; Yuan, C. L.; Lee, J. Y.; Archer, L. A. *Adv. Mater.* **2006**, *18*, 2325.
(3) Yang, H. G.; Zeng, H. C. *Angew. Chem., Int. Ed.* **2004**, *43*, 5930.
(4) Zhong, Z.; Yin, Y.; Gates, B.; Xia, Y. *Adv. Mater.* **2000**, *12*, 206.
(5) Sun, X.; Li, Y. *Anew. Chem., Int. Ed.* **2004**, *43*, 597.
(6) Titirici, M. M.; Antonietti, M.; Thomas, A. *Chem. Mater.* **2006**, *18*, 3808.
(7) Idota, Y.; Kubota, T.; Matsufuji, A.; Maekawa, Y.; Miyasaka, Y. *Science* **1997**, *176*, 1395.
(8) Ferrere, S.; Zaban, A.; Gregg, B. A. *J. Phys. Chem. B* **1997**, *101*, 4490.
(9) Law, M.; Kind, H.; Kim, F.; Messer, B.; Yang, P. *Angew. Chem., Int. Ed* **2002**, *41*, 2405.
(10) Wang, Y. L.; Jiang, X. C.; Xia, Y. N. *J. Am. Chem. Soc.* **2003**, *125*, 16176.
(11) Cheng, B.; Russell, J. M.; Shi, W. S.; Zhang, L.; Samulski, E. T. *J. Am. Chem. Soc.* **2004**, *126*, 5972.
(12) Zhao, L.; Yosef, M.; Steinhart, M.; Goring, P.; Hofmeister, H.; Gosele, U.; Schlecht, S. *Angew.Chem., Int. Ed.* **2005**, *45*, 311.
(13) Pan, Z. W.; Dai, Z. R.; Wang, Z. L. *Science* **2004**, *291*, 1947.
(14) Caruso, F.; Caruso, R. A.; Mohwald, H. *Science* **1998**, *282*, 1111.
(15) Dinsmore, A. D.; Hsu, M. F.; Nikolaides, M. G.; Marquez, M.; Bausch, A. R.; Weitz, D. A. *Science* **2002**, *298*, 1006.
(16) Sun, Y. G.; Xia, Y. N. *Science* **2002**, *298*, 2176.
(17) Yin, Y. D.; Rioux, R. M.; Erdonmez, C. K.; Hughes, S.; Somorjai, G. A.; Alivisatos, A. P. *Science* **2004**, *304*, 711.
(18) Liu, Y.; Dong, J.; Liu, M. L. *Adv. Mater.* **2004**, *16*, 353.

10.1021/cm7030575 CCC: $40.75
Published on Web 02/19/2008

oped based on the following understandings: It is known that carbonization of carbohydrates (e.g, glucose and sucrose) occurs under solvothermal conditions at temperatures above 160 °C.[5,6] On the other hand, hydrolysis of tin(IV) chloride ($SnCl_4$) under solvothermal conditions could lead to SnO_2 nanocrystals.[11] These properties of glucose and tin(IV) chloride were utilized in this study to enable first the in situ formation of mesospheres of carbon−SnO_2 nanocomposites. Carbon in the nanocomposites was then removed by calcination, leaving behind hollow core–shell mesospheres of crystalline SnO_2 nanoparticle aggregates. In this method, the in situ formed carbon-dominant mesospheres guided the organization of the final product morphology during the template removal process (calcination). Such a constructive role contrasts strongly with the destructive effect of template removal on product morphology common in other template-assisted methods. This preparation method is also environmentally benign and could be scaled up easily for volume production. When used as the anode material in lithium ion test batteries, the hollow core–shell mesospheres of crystalline SnO_2 nanoparticle aggregates demonstrated very high Li^+ storage capacities and improved electrochemical characteristics, which could all be attributed to their unique nanoarchitecture.

Experimental Section

Materials Synthesis and Characterization. All chemicals were used as received. In a typical experiment, 10 mmol of D-glucose monohydrate and 4 mmol of $SnCl_4$ were dissolved in a mixture of distilled water (5 mL) and ethanol (30 mL) to form a transparent colorless solution. The solution was transferred to a Teflon-lined autoclave. The autoclave was put in an electric oven and kept at 180 °C for 24 h before it was cooled in air. The sediment, which was black, was collected and washed with water and ethanol several times, before it was dried in a vacuum oven at 50 °C for a few hours. The sediment was then calcined at 550 °C for 4–5 h in air. The black sediment turned white indicating the successful removal of carbon by oxidization in air. The samples were characterized by field-emission scanning electron microscopy and scanning transmission electron microscopy (FESEM/STEM) on a JEOL JSM-6700F operating at 5 kV, by scanning electron microscopy and energy-dispersive X-ray spectroscopy (SEM/EDX) on a JEOL JSM-840 operating at 15 kV, by transmission electron microscopy and selected area electron diffraction (TEM/SAED) on a JEOL JEM-2010F operating at 200 kV, by powder X-ray diffraction (XRD) on a Shimadu XRD-6000 using Cu Kα radiation, and by X-ray photoemission spectroscopy on a KRATOS AXIS Hsi with Al Kα radiation.

Electrochemical Measurements. The hollow core–shell mesospheres of crystalline SnO_2 nanoparticle aggregates (80 wt %), conducting additive (10 wt %, Super-P carbon black, Timcal), and polyvinylidene fluoride (10 wt %, PVDF) binder in *N*-methylpyrrolidone (NMP) were mixed into a homogeneous slurry. The slurry was then applied to a copper disk current collector and dried in vacuum at 120 °C. Electrochemical test cells were assembled in an argon-filled glovebox using the coated copper disk as the working electrode, lithium metal foil as the counter/reference electrode, and 1 M solution of $LiPF_6$ in a 50:50 w/w mixture of ethylene carbonate (EC) and diethyl carbonate (DEC) as the electrolyte. The cells were charged and discharged galvanostatically at the rates of 50 or 100mA/g in the fixed voltage window from 5 mV to 2 V on a Maccor series 2000 battery tester at room temperature.

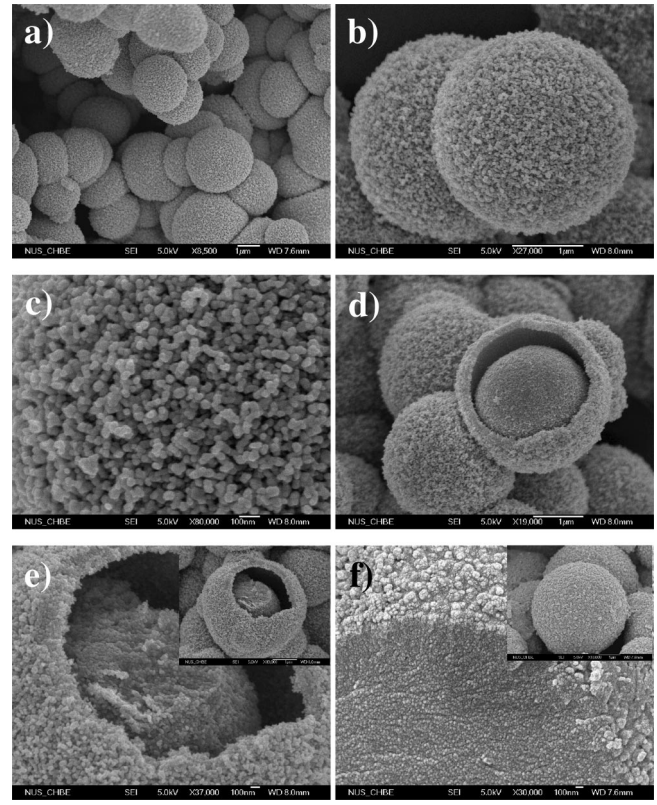

Figure 1. FESEM images: (a−b) hollow core–shell mesospheres of crystalline SnO_2 nanoparticle aggregates at different magnifications, (c) zoomed-in view of the surface of a SnO_2 mesosphere showing aggregates of SnO_2 nanoparticles, (d) a SnO_2 mesosphere with broken shell revealing the hollow core–shell structure, (e) zoomed-in view of another partially broken mesosphere showing that both the core and shell were made up of nanoparticle aggregates (the inset is the corresponding low-magnification view), and (f) zoomed-in and zoomed-out (inset) views of the solvothermal product of carbon mesospheres loaded with SnO_2 nanoparticles before calcination.

Results and Discussion

The FESEM images of the hollow core–shell mesospheres of crystalline SnO_2 nanoparticle aggregates are shown in Figure 1a−e at different magnifications. It is clear from Figure 1a that the mesospheres were 1–3 μm in overall dimension. The high magnification FESEM image of Figure 1b shows that the surface of the mesospheres was formed entirely by aggregated small (∼11 nm) primary SnO_2 nanoparticles. The zoomed-in view of the surface (Figure 1c) confirms this. The most unique feature of these SnO_2 mesospheres was their hollow core–shell structure, which was revealed most vividly by a mesosphere with partially broken shell (Figure 1d). The shell was estimated to be ∼200 nm in thickness. Another core–shell SnO_2 mesosphere with a ruptured shell is shown in Figure 1e. In addition to the shown annular space associated with the interior cavity, the core was found to be made up of the same aggregated SnO_2 nanoparticles as those found in the shell.

The interesting nanostructure of hollow core–shell mesospheres was further corroborated by transmission electron microscopy (TEM). The low-magnification TEM image in Figure 2a shows several core–shell mesospheres with clearly visible hollow interiors. The high-magnification TEM images, b and c of Figure 2, show an isolated SnO_2 mesosphere at different magnifications. The dark solid core of the

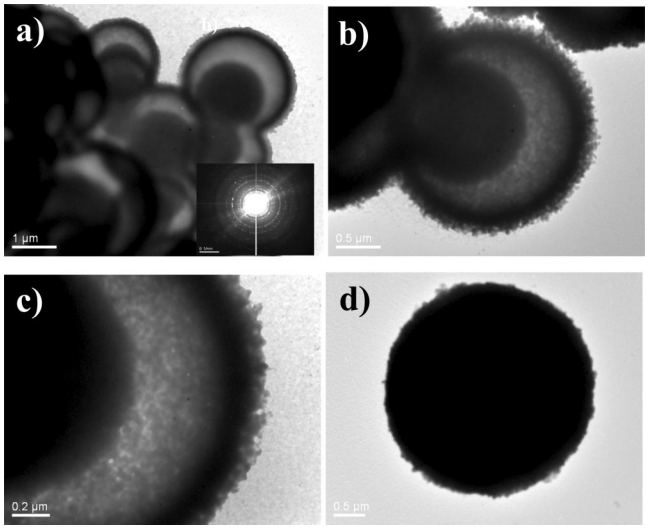

Figure 2. (a, b, c) TEM images of hollow core–shell mesospheres of crystalline SnO_2 nanoparticle aggregates at different magnifications. The cores were all solid. The inset in a shows the selected area diffraction pattern (SEAD) of a SnO_2 mesosphere, and d shows a TEM image of the solvothermal reaction product.

nanoparticle aggregate contrasts strongly with the visibly lighter region in the microvoid region between the core and the shell. The measured shell thickness of ~200 nm is consistent with the FESEM determination. The selected area diffraction pattern (SAED) of the SnO_2 mesospheres in the inset of Figure 2a indicates that the SnO_2 nanoparticles were crystalline, and all diffraction rings could be indexed to SnO_2 nanocrystals with hexagonal symmetry.

The crystallinity of the hollow core–shell mesospheres of SnO_2 nanoparticle aggregates was independently confirmed by X-ray diffraction (XRD). All the peaks in the XRD pattern (A.C) in Figure 3a could be indexed to crystalline SnO_2 by comparison with JCPDS card No. 41–1445, indicating good phase purity and consistency with the SAED measurement (inset in Figure 2a). The broad diffraction peaks indicate that the crystalline SnO_2 nanoparticles were small in size. If the {110} diffraction was used in the Scherrer equation ($D_v = K\lambda/(\beta \cos \theta$, where $K = 0.9$, β is the half-width of full maximum of the (110) peak, and $\lambda = 0.154$ nm), the size of the primary SnO_2 nanoparticles in the hollow core–shell mesospheres was determined to be ~11 nm, which is in good agreement with the measurement based on FESEM/TEM images. Elemental analysis by energy-dispersive X-ray spectroscopy (EDX) revealed the presence of only Sn and O (spectrum (A.C) in Figure 3b) in ~1:2 mole ratio, thereby confirming the sole presence of SnO_2. The hollow core–shell mesospheres of crystalline SnO_2 nanoparticle aggregates were further characterized by X-ray photoemission spectroscopy (XPS). The XPS spectrum for the Sn 3d levels is shown as curve A.C in Figure 3c. The two peaks at ~487.3 and ~495.6 eV could be assigned to Sn $3d_{5/2}$ and $3d_{3/2}$, respectively. The XPS data further proved the phase purity of the hollow core–shell mesospheres and that tin was in the Sn(IV) state.

To understand how the hollow core–shell mesospheres were formed, the black sediment after solvothermal synthesis before calcination (B.C) was collected and compared with the final product formed after calcination (A.C). The inset

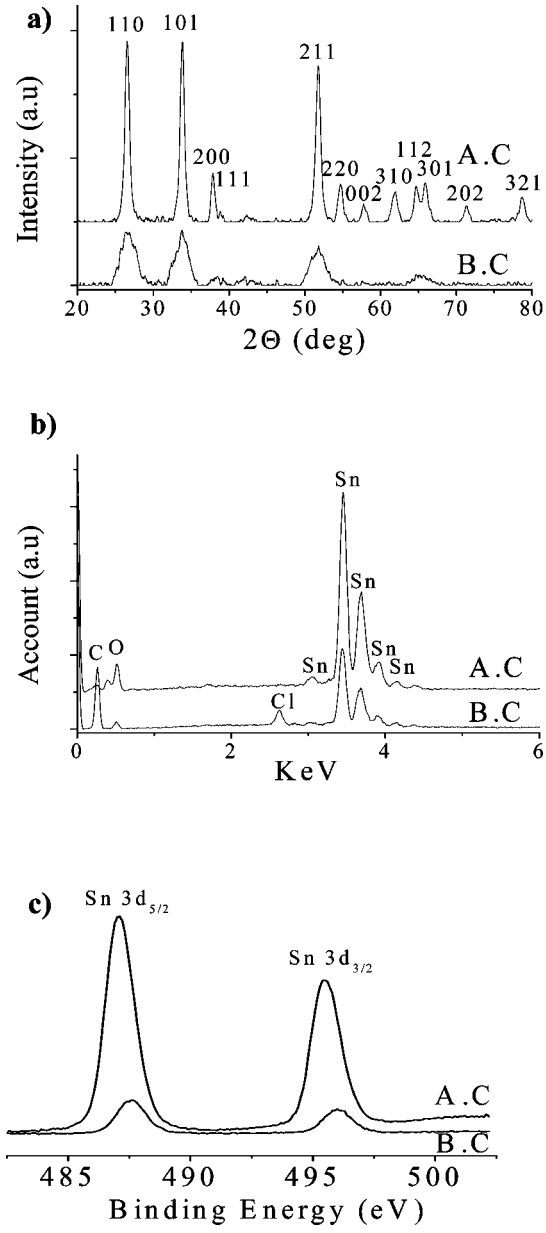

Figure 3. (a) XRD patterns, (b) EDX patterns, and (c) Sn 3d XPS spectra of the SnO_2 nanoparticle loaded carbon mesospheres prepared from the solvothermal reaction (B.C = before calcination) and hollow core–shell mesospheres of crystalline SnO_2 nanoparticle aggregates formed upon calcination (A.C = after calcination).

in Figure 1f shows the solvothermal product as carbon mesospheres with interspersed SnO_2 nanoparticles. The zoomed-in view of a broken carbon mesosphere (Figure 1f) indicates the clear presence of SnO_2 nanoparticles (white spots) on the carbon mesosphere external surface and throughout the ruptured cross-section of the mesosphere. Figure 2d shows a completely dark particle with no contrast difference between the surface and the particle interior, suggesting that the particle was entirely solid. The XRD pattern (B.C) in Figure 3a confirms the presence of SnO_2 nanocrystals. A nanocrystal size of ~3.5 nm was calculated based on the Scherrer equation using the {110} diffraction. The increase in the SnO_2 nanoparticle size after calcination could be the result of annealing, aggregation, and sintering of small particles (~3.5 nm) to form larger (~11 nm), more crystalline particles (see the sharper and narrower diffraction

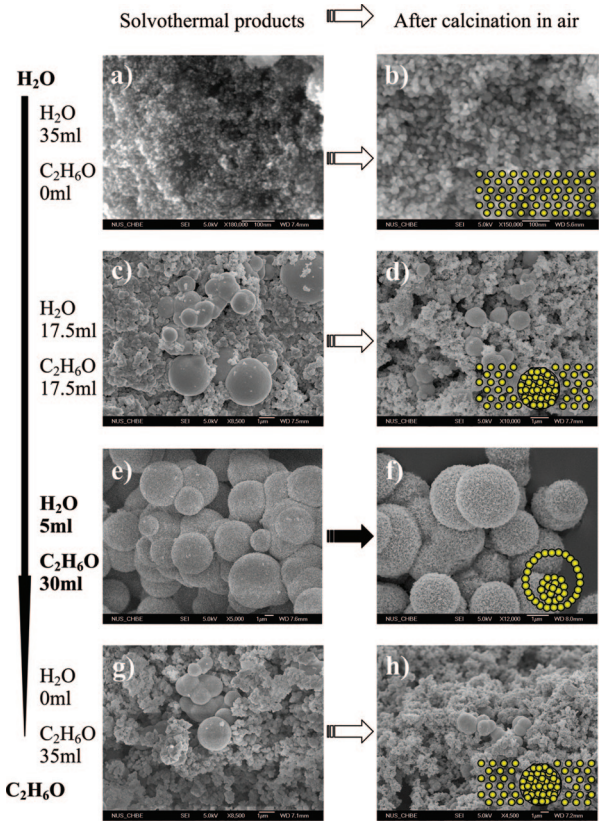

Figure 4. FESEM images of solvothermal products before (left panel) and after (right panel) calcination. The amount of ethanol used in the synthesis increased from a to g. It can be seen that the final product morphology was determined by the morphology of the solvothermal product.

peaks in pattern (A.C) of Figure 3a). The absence of carbon diffraction in pattern (B.C) indicates that the carbon spheres were amorphous.[5] As expected, the EDX pattern (B.C) of the sediment in Figure 3b detected the presence of carbon, in addition to tin, oxygen, and a trace amount of chlorine. The loss of carbon signal in the EDX pattern (A.C) in Figure 3b indicates that carbon was completely removed by oxidization in air. The XPS Sn 3d level spectrum (B.C.) in Figure 3c indicates that tin was in the Sn^{4+} oxidation state after solvothermal reaction. Thus it may be concluded that the distribution of SnO_2 nanoparticles in the carbon mesosphere was uniform throughout.

A series of experiments (summarized in Table 1 and Figure 1 in Supporting Information) was used to determine the key factors in solvothermal synthesis that led to the formation of the hollow core–shell product of SnO_2 nanoparticle aggregates. It was found that in water-rich solvent systems (ethanol/water = 0:35 or 5:30 mL), only SnO_2 nanoparticles surrounded by amorphous carbon were observed by the solvothermal reaction (Figure 4a), and subsequent calcination treatment led to crystalline SnO_2 nanoparticles only (Figure 4b). When the ethanol content in the mixed solvent was increased to ethanol/water = 17.5:17.5 mL, both SnO_2 nanoparticles surrounded by amorphous carbon and SnO_2 nanoparticle-loaded carbon mesospheres were formed (Figure 4c). Subsequent calcination led to a mixture of SnO_2 nanoparticles and mesospheres of SnO_2 nanoparticle aggregates (Figure 4d). Nearly identical results were obtained in an entirely ethanol system (ethanol/water = 35:0 mL) (Figure 4g and h). *The SnO_2 mesospheres in these cases were all solid nanoparticle aggregates*. The discovery of all-solid mesospheres of crystalline SnO_2 nanoparticle aggregates actually attested to the uniformity of dispersion of SnO_2 nanoparticles in the carbon mesospheres. The lack of a hollow interior in these cases could be caused by the excess presence or oversupply of SnO_2 nanoparticles in the mesospheres, which was witnessed by the presence of a large number of discrete SnO_2 nanoparticles in the proximity of the SnO_2 mesospheres. The hollow core–shell mesospheres of SnO_2 nanoparticle aggregates could only be produced from a solvent mixture of ethanol/water = 30:5 mL (Figure 4e−f). These experimental results demonstrated that (1) ethanol could have affected the polarity of the solvent system and hence the solubility of reactants and intermediates in solvothermal synthesis and that (2) the product morphology mirrored closely the morphology of the solvothermal product formed before calcination and was little affected by the calcination process. In other words, the carbon product from the carbonization of glucose (mostly amorphous carbon) templated the formation of crystalline SnO_2-only nanoparticle aggregates upon calcination.

Under solvothermal conditions, the two reactions (hydrolysis of $SnCl_4$ and carbonization of glucose) occurred simultaneously. Since glucose was used in large excess, the hydrolysis and ethanolysis of $SnCl_4$ occurred within the microenvironment of glucose dehydration and polymerization (carbonization), and the SnO_2 nanoparticles formed thereupon served as the nucleation sites for amorphous carbon deposition. The amorphous carbon surface was hydrophilic (because of the presence of −OH or ═C═O groups), and the aggregation of the carbon coated SnO_2 nanoparticles was strongly dependent on the solvent properties, in particular the water/ethanol ratio. Under the condition of high water content, the carbon-coated SnO_2 nanoparticles were well solubilized, and aggregation was limited (Figure 4a). The interparticle aggregation increased with the ethanol content (Figure 4c), and under the right mix of ethanol and water, the particles aggregated into mesospheres exclusively (Figure 4e). At high ethanol content, where glucose was not fully solubilized, while $SnCl_4$ was completely dissolved, the local dehydration and carbonization of glucose and $SnCl_4$ hydrolysis could not occur uniformly throughout, and a heterogeneous product consisting of carbon mesospheres loaded with SnO_2 nanoparticles, and carbon coated SnO_2 nanoparticles was formed (Figure 4g).

On the basis of the experimental evidence, the schematic illustration in Scheme 1 was proposed to rationalize the changes in material constitution and morphology during solvothermal synthesis and postsynthesis calcination. Under solvothermal conditions with a solvent with the right polarity and solubilization power (obtained by adjustment of the amounts of ethanol and water used), only carbon mesospheres loaded with SnO_2 nanoparticles were formed in the solvothermal reaction. Upon calcination in air, the carbon in the mesospheres was oxidized to CO_2, and the SnO_2 nanoparticles annealed to higher crystallinity. The outward diffusion of CO_2 generated a force to compress the SnO_2 nanoparticles in the surface region into a shell.[1] The shell

Scheme 1. Schematic Illustration of the Compositional and Morphological Evolutions in Solvothermal Synthesis and Postsynthesis Calcination in Air

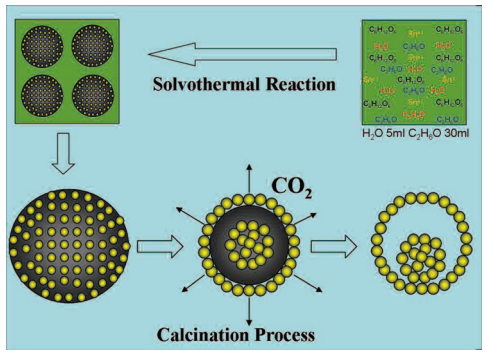

continued to anneal in the process and formed a thermally stable structure. The mesoporous shell would still allow carbon dioxide effusion from the regions below the shell, but probably at a slower rate. A stable core was eventually formed by the compaction and annealing of SnO_2 nanoparticles in the mesosphere core region because of the shrinking carbon core. Collectively this had led to the formation of hollow core–shell mesospheres consisting entirely of aggregates of crystalline SnO_2 nanoparticles. The amorphous carbon-dominant mesospheres first formed as the solvothermal product were instrumental in crafting the final product geometry. While we have additional experimental evidence supporting the product morphology development according to this phenomenological model (Supporting Information), more work is still needed to validate the individual steps.

The hollow core–shell mesospheres of crystalline SnO_2 nanoparticle aggregates were evaluated as a potential anode material for the lithium ion batteries. In theory, SnO_2 could store close to three times the amount of lithium ions in conventional graphite anodes because of the ability of Sn to alloy with lithium to a stoichiometry of $Li_{4.4}Sn$

$$SnO_2 + 44Li^+ + 4e^- \rightarrow Sn + 2Li_2O \quad (1)$$

$$Sn + xLi^+ + xe^{-1} \leftrightarrow Li_xSn \quad (0 \le x \le 4.4) \quad (2)$$

The experimental values for the first cycle charge (Li^+ *insertion*) and discharge (Li^+ *extraction*) capacities were very high, at 2358 and 1303 mAh/g, respectively, when measured at the current density of 50 mA/g (Figure 5a). The exceptionally high first-cycle charge capacity could be attributed to solid−electrolyte interphase (SEI) formation and the reduction of SnO_2 to Sn (reaction 1).[1,2,19,20,24] In addition the micropores in the mesosphere core and shell were also a facility for Li^+ storage.[19] The Li^+ stored in these locations were, however, more difficulty to extract, accounting for the apparently large disparity between charge and discharge

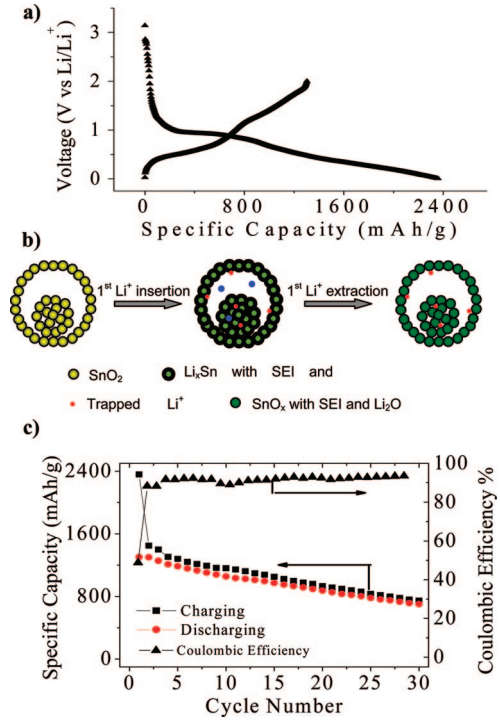

Figure 5. (a) First cycle charging/discharging profiles. (b) Schematic showing the processes occurring in the first cycle of Li^+ insertion and extraction. (c) Specific capacity vs cycle number plots of electrodes prepared from the hollow core–shell mesospheres of crystalline SnO_2 nanoparticle aggregates. Test conditions: current density = 50mA/g, voltage window = 5mV−2V.

capacities (Figure 5b). The quasi-reversible reaction between Li_2O and Sn to reform SnO_2 could be another likely source for the high discharge capacity.[20] Both the core and shell components of the mesospheres are expected to contribute to the high capacities because the core was electrochemically accessible through physical contact with the shell. This was especially so after conductivity was increased by converting semiconducting SnO_2 into metallic Sn and the alloying of Sn with Li to form Li_xSn alloys. Figures 5c shows the cycling performance of the SnO_2 mesospheres. Even at the rate of 100 mA/g, the specific charge and discharge capacities at the end of 30 cycles were still comparable to the theoretical capacity of SnO_2 (Figure 2 of SI). Examination of the electrode after 76 cycles indicated at least partial retention of the mesosphere morphology, although most of the hollow core–shell SnO_2 mesospheres had collapsed with noticeable aggregation of the Sn/SnO_2 nanoparticles (Figure 3 of SI). Since capacity fading was still prominent in these hollow core–shell mesospheres of crystalline SnO_2 nanoparticle aggregates, the current morphological modification has rectified some, but not all, of the SnO_2 deficiencies in applications.

Conclusion

In summary, crystalline SnO_2 nanoparticles were successfully assembled into a high-order nanostructure of hollow core–shell mesospheres by a simple and environmentally benign procedure consisting of solvothermal synthesis and postsynthesis calcination. Carbon mesospheres laden with crystalline SnO_2 nanoparticles were formed, using a suitably formulated water/ethanol mixture, as the sole product of solvothermal synthesis from tin

(19) Winter, M.; Besenhard, J. O. *Electrochim. Acta* **1999**, *45*, 31.
(20) Sun, X.; Liu, J.; Li, Y. *Chem. Mater.* **2006**, *18*, 3486.
(21) Poizot, P.; Laruelle, S.; Grugeon, S.; Dupont, L.; Tarascon, J. M. *Nature* **2000**, *407*, 496.
(22) Arico, A. S.; Bruce, P.; Scrosati, B.; Tarascon, J. M.; Schalkwijk, W. V. *Nat. Mater.* **2005**, *4*, 366.
(23) Tarascon, J. M.; Armand, M. *Nature* **2000**, *414*, 359.
(24) Kim, C.; Noh, M.; Choi, M.; Cho, J.; Park, B. *Chem. Mater.* **2005**, *17*, 3297.

and carbon precursors. Subsequent calcination compressed the SnO_2 nanoparticles into hollow core–shell mesospheres. The carbon in the mesospheres played the constructive role of templating the final product morphology during the carbon removal process. This unique SnO_2 nnaostructure could store an exceedingly large amount of Li^+, and cycled well for a phase-pure SnO_2 anode.

Supporting Information Available: Table of other experimental conditions and the corresponding scheme of results, testing results at current rate of 100 mA/g, and morphology after more than 76 cycles of charge and discharge. This material is available free of charge via the Internet at http://acs.org.

CM7030575